A Split Hopkinson Bar Technique to Determine Compressive Stress-Strain Data for Rock Materials

by D. J. Frew, M. J. Forrestal and W. Chen

ABSTRACT- We present a split Hopkinson pressure bar technique to obtain compressive stress-strain data for rock materials. This technique modifies the conventional split Hopkinson bar apparatus by placing a thin copper disk on the impact surface of the incident bar. When the copper disk is impacted by the striker bar, a nondispersive ramp pulse propagates in the incident bar and produces a nearly constant strain rate in a rock sample. Data from experiments with limestone show that the samples are in dynamic stress equilibrium and have constant strain rates over most of the duration of the tests. We also present analytical models that predict the time durations for sample equilibrium and constant strain rate. Model predictions are in good agreement with measurements.

D. J. Frew is Research Engineer, U.S. Army Engineer Research and Development Center, Structures Laboratory, at the Waterways Experiment Station, *Vicksburg, MS 39180-6199. M. J. Forrestal is Distinguished Member of Technical Staff, Sandia National Laboratories, Albuquerque, NM 87185-0303. W. Chen is Assistant Professor, Department of Aerospace and Mechanical Engineering, University of Arizona, Tucson, AZ 85721-0119.*

DISCLAIMER

Introduction

The split Hopkinson pressure bar (SHPB) technique originally developed by Kolsky[1, 2] has been used by many investigators to obtain dynamic compression properties of solid materials. This technique has mostly been used to study the plastic flow stress of metals that undergo large strains at strain rates between $10^2 - 10^4$ s^{-1}. The evolution of this experimental method and recent advances are discussed by Nicholas[3], Follansbee[4], Nemat-Nasser, Isaacs, and Starrett[5], Ramesh and Narasimha[6], Gray[7], and Gray and Blumenthal.[8] As discussed by Yadav, Chichili, and Ramesh[9], data for the compressive flow stress of metals are typically obtained for strains larger than a few percent because the technique is not capable of measuring the elastic and early yield behavior. By contrast, most of the material behavior of interest for relatively brittle materials such as ceramics and rocks occurs at strains less than about 1.0 percent.

In this study, we modified the conventional split Hopkinson pressure bar or Kolsky bar technique to obtain dynamic compressive, stress-strain data for rock materials and conducted experiments with limestone samples that have failure strains less than 1.0 percent. The analytical and experimental work presented in this study for rock materials uses and extends recently published work for ceramic materials. We particularly cite the experimental and analytical work by Nemat-Nasser, Isaacs, and Starrett[5] for pulse shaping and the sample equilibrium model published by Ravichandran and Subhash.[10]

For an ideal Kolsky compression bar experiment, the sample should be in equilibrium and should deform at a constant strain rate over most the duration of the test. To closely approximate these ideal conditions for experiments with brittle ceramic and rock materials, a properly designed, thin copper disk is placed on the impact surface of the incident bar so that a nondispersive ramp pulse propagates in the incident bar. Data from experiments presented in this study show that limestone samples were in equilibrium and at constant strain rates over most

of the duration of the tests. Thus, a pulse shaping technique is an essential modification in order to closely approximate these ideal test conditions. Experiments that attempt to obtain stress-strain data for ceramic materials at constant strain rates are reported by Rogers and Nemat-Nasser[11] and Chen and Ravichandran.[12] While we were able to use many of the contributions from the published papers on ceramic materials, several new modifications were required for our Kolsky pressure bar experiments with rock materials. For example, compressive strengths for ceramics are more than a factor of ten larger than compressive strengths for limestone, so the limestone sample diameters were the same as the bar diameters. More importantly, in order to obtain sample equilibrium, a pulse shaper must be designed to produce a much smaller slope on the ramp pulse propagating in the incident bar because the wave speed for limestone is three to four times smaller than typical wave speeds for ceramics. Other critical experimental modifications are discussed in the following sections.

Split Hopkinson Pressure Bar (SHPB) or Kolsky Bar

As shown in Fig. 1, a conventional split Hopkinson pressure bar (SHPB) consists of a striker bar, an incident bar, a transmission bar, and a sample placed between the incident and transmission bars. A gas gun launches the striker bar at the incident bar and that impact causes an elastic compression wave to travel in the incident bar towards the sample. When the impedance of the sample is less than that of the bars, an elastic tensile wave is reflected into the incident bar and an elastic compression wave is transmitted into the transmission bar. If the elastic stress pulses in the bars are nondispersive, the elementary theory for wave propagation in bars can be used to calculate the sample response from measurements taken with strain gages mounted on the incident and transmission bars. Strain gages mounted on the incident bar

measure the incident ε_i and reflected ε_r strain pulses, and strain gages mounted on the transmission bar measure the transmitted ε_t strain pulse. Nicholas[3], Follansbee[4], and Gray[7] present equations that describe the sample response in terms of the measured strain signals.

For this study the incident and transmission bars were made from the same material with equal cross-sectional areas. As shown in Fig. 1, the bars have density ρ, Young's modulus E, bar wave speed c, and cross-sectional area A. Since we only focus on limestone samples that have failure strains less than 1.0 percent, we need only use engineering stress, strain, and strain-rate measures. In addition, we take stress positive in compression, strain positive in contraction, and particle velocity positive to the right in Fig. 1. Figure 1 also shows the sample has cross-sectional area A_s and length l_o. We take subscripts 1 and 2 to represent the locations of the ends of the sample.

Strain rate of the sample is given by

$$\frac{d\varepsilon_s}{dt} = \frac{v_1 - v_2}{l_o}, \tag{1}$$

where v_1 and v_2 are the particle velocities at the sample and bar interfaces. In terms of the measured strain pulses

$$\frac{d\varepsilon_s}{dt} = \frac{c}{l_o}(\varepsilon_i - \varepsilon_r - \varepsilon_t). \tag{2}$$

Forces at the ends of the sample are

$$P_1 = EA(\varepsilon_i + \varepsilon_r) \tag{3a}$$

$$P_2 = EA\varepsilon_t \tag{3b}$$

and the average force is

$$P_a = \frac{EA}{2}(\varepsilon_i + \varepsilon_r + \varepsilon_t). \tag{3c}$$

Similarly, stresses at the ends of the sample are

$$\sigma_1 = \frac{EA}{A_s}(\varepsilon_i + \varepsilon_r) \tag{4a}$$

$$\sigma_2 = \frac{EA}{A_s}\varepsilon_t \tag{4b}$$

and the average sample stress is

$$\sigma_a = \frac{EA}{2A_s}(\varepsilon_i + \varepsilon_r + \varepsilon_t). \tag{4c}$$

If $P_1=P_2$, the forces on both ends of the sample are equal, and from eqs (3a) and (3b) $\varepsilon_i + \varepsilon_r = \varepsilon_t$. So if the sample is in dynamic stress equilibrium, the stress, strain rate, and strain are given by

$$\sigma_s = \frac{EA}{A_s}\varepsilon_t \tag{5}$$

$$\frac{d\varepsilon_s}{dt} = \frac{-2c}{l_o}\varepsilon_r \tag{6}$$

$$\varepsilon_s = \frac{-2c}{l_o}\int_0^t \varepsilon_r(\tau)\, d\tau. \tag{7}$$

As discussed in detail by Ravichandran and Subash[10], Gray[7], and Gray and Blumenthal[8], eqs (5), (6), and (7) assume that the sample is in dynamic stress equilibrium. Equilibrium should first be examined by comparing the stresses σ_1 and σ_2 at the ends of the sample given by eqs (4a) and (4b). If σ_1 and σ_2 are in reasonable agreement, only then it is reasonable to use eqs (5), (6), and (7) to calculate sample stress, strain rate, and strain.

A Conventional SHPB or Kolsky Bar Experiment

We present results from a conventional SHPB experiment with an Indiana limestone sample (Elliot Stone Company, Bedford, IN). Pettijohn[13], and Podnieks, Chamberlain, and Thill[14] describe this limestone as a carbonate rock that contains over 90 percent calcite and less than 10 percent quartz, has a porosity of about 15 percent, and a grain size ranging between 0.15 and 1.0 mm. For this study, the limestone samples had density ρ_s = 2300 kg/m^3, Young's modulus E_s = 24 GPa, and bar wave velocity c_s = 3200 m/s. Young's modulus was estimated from quasi-static compression data shown later. In addition, the sample had a length and diameter of 12.7 mm, and the sample and bar diameters were equal.

The striker, incident, and transmission bars shown in Fig. 1 had lengths of 152 mm, 2130 mm, and 915 mm, respectively. The bars were made from high strength, maraging VM350 steel (Vasco Pacific, Montebello, CA) and have density ρ = 8100 kg/m^3, Young's modulus E = 200

GPa, and bar wave velocity c = 4970 m/s. The strain gages shown in Fig.1 are located at 1060 mm from the impact surface on the incident bar and 229 mm from the sample/ bar interface on the transmission bar.

Figure 2 shows incident, reflected, and transmitted strain-time signals for a striking velocity of 8.05 m/s. The incident pulse has a fast rise time of about 10 μs and a pulse width of about 60 μs that corresponds to two wave transit times in the striker bar. Figure 3 shows stress versus time at the ends of the sample calculated from eqs (4a) and (4b) and the average strain rate calculated from eq (2). For an ideal SHPB experiment, the sample should be in equilibrium and should deform at a constant strain rate over most of the duration of the test. However, Fig.3 shows that σ_1 and σ_2 are not in close agreement and that the strain rate is not constant over the duration of the test.

In the next sections, we present models and experimental results that show a ramp incident pulse is required to obtain sample equilibrium and constant strain rate over most of the test duration. The ramp incident pulse is produced by placing a thin copper disk on the impact surface of the incident bar. We describe the details of this pulse shaping technique in another study.[15]

Models for Sample Equilibrium and Constant Strain Rate

In this section, we develop models that show the evolutionary process for sample equilibrium and constant strain rate for brittle materials that have a linear stress-strain response until failure. These models and subsequent experiments show that a ramp stress pulse in the incident bar is required in order to obtain sample equilibrium and constant strain rate over most of the duration of the experiment. The first model assumes that the sample is in stress

equilibrium and predicts strain and strain rate versus time. For the second model, we perform a wave propagation analysis on the interaction of the sample with the incident and transmission bars. This second model predicts the stress-time histories on either side of the sample.

A ramp pulse propagates in the incident bar given by

$$\sigma_i(x, t) = M(t - \frac{x}{c}) \cdot H(t - \frac{x}{c}) \tag{8}$$

where H is the Heaviside unit function and M is the stress loading rate. We take x = 0 at the interface between the incident bar and the sample labeled as station 1 in Fig. 1. If the sample is in equilibrium, $\sigma_1 = \sigma_2$, and we neglect wave propagation in the sample. The sample is assumed to have a linear stress-strain response to failure given by

$$\sigma_s = E_s \, \varepsilon_s \, . \tag{9}$$

where E_s is the Young's modulus for the sample.

When the incident stress pulse reaches the sample, stress pulses are reflected back into the incident bar and transmitted into the transmission bar. As before, we take stress positive in compression, strain positive in contraction, and particle velocity positive to the right in Fig. 1. From the equations of elementary bar theory[16], strain rate in the sample given by eq (1) can be written in terms of the incident σ_i, reflected σ_r, and transmitted σ_t stress pulses in the bars as

$$\frac{d\varepsilon_s}{dt} = \frac{1}{\rho c l_o}(\sigma_i - \sigma_r - \sigma_t). \tag{10}$$

For a sample in equilibrium, $\sigma_i + \sigma_r = \sigma_t$, and

$$\frac{d\varepsilon_s}{dt} = \frac{2}{\rho c l_o}(\sigma_i - \sigma_t). \tag{11}$$

The incident and transmitted stresses in the bars are

$$\sigma_i = Mt \tag{12a}$$

$$\sigma_t = \frac{A_s E_s \varepsilon_s}{A}. \tag{12b}$$

From eqs (11) and (12),

$$\frac{d\varepsilon_s}{dt} + \frac{2A_s E_s}{\rho c A l_o}\varepsilon_s = \frac{2Mt}{\rho c l_o} \tag{13}$$

which has solutions

$$\frac{d\varepsilon_s}{dt} = \frac{\gamma M}{E_s}\left[1 - \exp\left(\frac{-2t}{r\,t_o}\right)\right] \tag{14a}$$

$$\varepsilon_s = \frac{\gamma M}{E_s}\left\{1 - \frac{r\,t_o}{2t}\left[1 - \exp\left(\frac{-2t}{r\,t_o}\right)\right]\right\} \tag{14b}$$

$$\gamma = \frac{A}{A_s}, \qquad r = \frac{A\,\rho\,c}{A_s\,\rho_s\,c_s}, \qquad t_o = \frac{l_o}{c_s}. \tag{14c}$$

Equations (14a) and (14b) give closed-form solutions for the strain rate and strain in the sample. However, this model assumes that the sample is in equilibrium.

For the second model, we perform a wave propagation analysis on the interaction of the sample with the incident and transmission bars. Ravichandran and Subash[10] present a method of characteristics solution for this problem and show results for ceramic materials. Our analysis of this same problem provides closed-form equations that we find more convenient for numerical applications.

We use the elementary theory of wave propagation in bars to calculate the stress-time histories at the ends of the sample. Ravichandran and Subash[10] and Graff[16] present equations for the reflected and transmitted stresses at the interfaces shown in Fig. 1. At the incident bar/ sample interface (location 1 in Fig. 1), the stresses transmitted to the specimen σ_t and reflected in the incident bar σ_r are

$$\sigma_t = \left(\frac{2\gamma}{r+1}\right)\sigma_i \tag{15a}$$

$$\sigma_r = -\left(\frac{(r-1)}{r+1}\right)\sigma_i \tag{15b}$$

in which r is given by eq (14c) and σ_i is the incident pulse given by eq (8). We take x = 0 at station 1 in Fig. 1, and the stress in the sample at station 1 is

$$\sigma_1 = \frac{2\gamma M t}{r+1}, \qquad 0 \le t < 2t_o. \quad (16)$$

At $t = t_o$, the stress wave in the sample reaches the sample/ transmission bar interface (location 2 in Fig. 1). When the stress wave in the sample travels toward station 2 and interacts with the transmission bar, the stresses transmitted into the transmission bar σ_t and reflected into the sample are

$$\sigma_t = \frac{2r\sigma_1}{\gamma(r+1)}, \qquad t_o \le t < 3t_o \quad (17a)$$

$$\sigma_r = \left(\frac{r-1}{r+1}\right)\sigma_1, \qquad t_o \le t < 3t_o \quad (17b)$$

where σ_1 is given by eq (16). The stress in the sample at station 2 consists of the incident and reflected stress waves and is given by

$$\sigma_2(t) = \frac{2\gamma M}{r+1}(t-t_o) + \left(\frac{r-1}{r+1}\right)\frac{2\gamma M}{r+1}(t-t_o), \quad t_o \le t < 3t_o. \quad (18)$$

We repeat this interaction process several times and obtain

$$\sigma_1 = \frac{2\gamma M t}{r+1}, \qquad 0 \le t < 2t_o \quad (19a)$$

$$\sigma_1 = \frac{2\gamma M}{r+1}\left\{t + \left[\left(\frac{r-1}{r+1}\right) + \left(\frac{r-1}{r+1}\right)^2\right](t-2t_o)\right\},\ 2t_o \le t < 4t_o \quad (19b)$$

$$\sigma_1 = \frac{2\gamma M}{r+1}\left\{t + \left[\left(\frac{r-1}{r+1}\right) + \left(\frac{r-1}{r+1}\right)^2\right](t-2t_o) + \left[\left(\frac{r-1}{r+1}\right)^3 + \left(\frac{r-1}{r+1}\right)^4\right](t-4t_o)\right\},$$
$$4t_o \le t < 6t_o \quad (19c)$$

and

$$\sigma_2 = 0, \qquad 0 \le t < t_o \quad (20a)$$

$$\sigma_2 = \frac{2\gamma M}{r+1}\left\{\left[1 + \left(\frac{r-1}{r+1}\right)\right](t-t_o)\right\}, \qquad t_o \le t < 3t_o \quad (20b)$$

$$\sigma_2 = \frac{2\gamma M}{r+1}\left\{\left[1 + \left(\frac{r-1}{r+1}\right)\right](t-t_o) + \left[\left(\frac{r-1}{r+1}\right)^2 + \left(\frac{r-1}{r+1}\right)^3\right](t-3t_o)\right\},$$
$$3t_o \le t < 5t_o. \quad (20c)$$

The nth term for eqs (19) and (20) is

$$\frac{2\gamma M}{r+1}\left[\left(\frac{r-1}{r+1}\right)^{n-1} + \left(\frac{r-1}{r+1}\right)^n\right](t-nt_o)$$

for the time interval $n\ t_o \leq t < (n+2)\ t_o$. Therefore, σ_1 and σ_2 can easily be calculated for times greater than those given by eqs (19) and (20).

Figures 4 and 5 show model predictions for sample stresses and strain rate versus time. These predictions correspond to experiments with steel bars and limestone samples ($r = 5.5$) and with equal sample and bar diameters ($\gamma = 1$). For Fig. 4, the stress loading rate in the incident bar (eq (8)) is $M = 3.3$ MPa/μs and corresponds to the loading rate for experiments discussed in the next section. In addition, the sample fails or starts to fail at a sample stress $\sigma_s > 120$ MPa. Figure 4 shows that the stresses at the incident bar/ sample interface σ_1 and the sample/ transmission bar interface σ_2 are nearly equal for $t/t_o > 2$. In addition, the sample stress predicted by the model that assumes sample equilibrium given by eqs (9) and (14b) lies between σ_1 and σ_2. The strain rate rapidly increases from $o < t/t_o < 4$ and is nearly constant for $4 < t/t_o < 12$, so the strain rate is nearly constant for a sample stress between about 20 and 120 MPa. Figure 5 shows model predictions for stresses and strain rate versus time for a stress loading rate of $M = 9.9$ MPa/μs. A comparison of the results in Figs. 4 and 5 show that as the loading rate increases from 3.3 to 9.9 MPa/μs, the interface stresses σ_1 and σ_2 begin to differ from each other and the strain rate varies significantly over most of the duration of the test.

Modified SHPB or Kolsky Compression Bar Experiments

Models developed in the previous section predict that a nondispersive ramp pulse in the incident bar is required for testing brittle materials that have a linear stress-strain responses to failure. To obtain the ramp pulse in the incident bar, we modify the conventional SHPB technique by placing a thin copper disk on the impact surface of the incident bar. Nemat-Nasser, Isaacs, and Starrett[5] present a pulse shaping model and data for oxygen-free, high purity copper

(C10200)[17]. In another study[15], we extend the model of Nemat-Nasser, Isaacs, and Starrett[5] and present data for both annealed and hardened C11000 copper[17] pulse shapers.

In this section, we present results from two experiments that demonstrate our modified SHPB technique. Data from experiments with limestone show that the samples are in dynamic stress equilibrium and have nearly constant strain rates over most of the duration of the tests. In addition, we carefully bracket sample failure with one test where the sample fails with catastrophic damage and a second test where the sample is recovered intact. These experiments used the same limestone samples described in the previous section, **A Conventional SHPB or Kolsky Bar Experiment**. The sample had a length and diameter of 12.7 mm, and the sample and bar diameters were equal. The high strength steel incident and transmission bars had lengths of 2130 and 915 mm, respectively. Strain gages shown in Fig. 1 are located at 1065 mm from the impact surface of the incident bar and 229 mm from the sample/ bar interface on the transmission bar. To obtain a nearly linear ramp pulse in the incident bar, a 3.97-mm-diameter, 0.79-mm-thick, annealed (C11000)[15, 17] copper disk was placed on the impact surface of the incident bar. All the above mentioned parameters remained fixed for the two experiments presented in this section. However, the first experiment used a 154-mm-long, steel striker bar, and the second experiment used a 51-mm-long, steel striker bar. Both striker bars were launched to a striking velocity of 13.9 m/s.

Figure 6 shows the measured incident stress pulse and a prediction from our model[15] for a 154-mm-long, steel striker bar with a striking velocity of 13.9 m/s. Note that the incident stress pulse is nearly a linear ramp for about 75 μs and has a stress loading rate of about M = 3.3 MPa/μs. Incident, reflected, and transmitted strain pulses presented in Fig. 7 show that the high frequency oscillations that appear in Fig. 2 are eliminated with pulse shaping. Thus, data

analyses that use the elementary bar theory should be more accurate for pulse shaped experiments. Figure 8 presents stresses in the sample at the incident bar/ sample interface σ_1 and the sample/ transmission bar interface σ_2 calculated from eqs (4a) and (4b) that use the measured strain signals. We also show that the model prediction from eqs (9) and (14b) are in good agreement with the measured stresses and that σ_1 and σ_2 are in close agreement. Thus, the sample is nearly in a state of dynamic stress equilibrium. Figure 8 also shows the predicted and measured strain rates versus time. Strain rate is nearly constant for $15\mu s < t < 50\ \mu s$. At about 50 μs, the limestone sample begins to fail. When failure starts, the sample is no longer in a state of homogeneous deformation and the valid range of the experiment is over. Post-test observations showed that the sample eventually experienced catastrophic damage.

Figures 6 and 8 show that the limestone sample started to fail at about 50 μs and the incident ramp pulse was loading for about 75 μs. Therefore, the sample continued to be loaded after the start of failure and the sample eventually experienced catastrophic damage. To recover an intact limestone sample after a test, we conducted another experiment with a ramp pulse in the incident bar with a shorter duration than the pulse shown in Fig. 6. Figure 9 shows the measured incident stress pulse and a prediction from our model[15] for a 51-mm-long, steel striker bar with a striking velocity of 13.9 m/s. Note that the incident stress pulse is nearly a linear ramp for about 50 μs and has a stress loading rate of about M = 3.1 MPa/μs. Thus the incident pulses shown in Figs. 6 and 9 are almost identical except for the loading durations of 75 μs and 50 μs, respectively. Results for the 50 μs ramp incident pulse are shown in Fig. 10 and are very similar to those presented in Fig. 8. However, the strain rate in Fig. 8 shows an exponential growth after about 50 μs, and the strain rate in Fig. 10 remains nearly constant. Thus the sample is loaded after failure began in the first experiment, and the loading ended at about the time the sample

started to fail in the second experiment. In the first experiment the limestone sample eventually failed with catastrophic damage; whereas, in the second experiment the sample was recovered intact. From Figs. 8 and 10 we conclude that the limestone sample has a failure stress of about 120 MPa for a strain rate between 100 s^{-1} and 120 s^{-1}.

In Fig. 11, we show stress-strain curves from the dynamic experiments discussed in this section and a quasi-static stress-strain curve. We note that the failure stress at a strain rate between 100 s^{-1} and 120 s^{-1} is about double that obtained from a quasi-static experiment.

Conclusions

We presented a modified split Hopkinson pressure bar or Kolsky bar technique to obtain compressive stress-strain data for rock materials. A nondispersive ramp pulse was produced in the incident bar by placing a thin copper disk on the impact surface of the incident bar. Data from experiments with limestone samples showed the samples were in dynamic stress equilibrium and had constant strain rates over most of the test durations. We also presented analytical models that predicted the time durations for sample equilibrium and constant strain rate.

Acknowledgements

This work was sponsored by the U.S. Army Engineer Research and Development Center (ERDC) at the Waterways Experiment Station under a laboratory director's discretionary research program and by the Sandia National Laboratories Joint DoD/ DOE Penetration Technology Program. Sandia is a multiprogram laboratory operated by Sandia Corporation, a Lockheed Martin Company, for the United States Department of Energy under Contract DE-AC04-94AL8500. The authors gratefully acknowledge permission from the Director, Structures Laboratory, ERDC to publish this work.

References

1. *Kolsky, H., "An Investigation of the Mechanical Properties of Materials at Very High Rates of Loading," Proc. Royal Soc. Lon., B, 62, 676-700, (1949).*

2. *Kolsky, H., Stress Waves in Solids. Dover, New York (1963).*

3. *Nicholas, T., " Material Behavior at High Strain Rates," Impact Dynamics, Chapter 8, John Wiley & Sons, New York, (1982).*

4. *Follansbee, P. S., "The Hopkinson bar," In Mechanical Testing, Metals Handbook, 9th ed., 8, American Society for Metals, Metals Park, Ohio, 198-217, (1985).*

5. *Nemat-Nasser, S., Isaacs, J. B. and Starrett, J. E., "Hopkinson Techniques for Dynamic Recovery Experiments," Proc. R. Soc. Lond., A, 435, 371-391,(1991).*

6. *Ramesh, K. T. and Narasimhan, S., "Finite Deformations and the Dynamic Measurement of Radial Strains in Compression Kolsky Bar Experiments," Int. J. Solids Structures, 33, 3723-3738, (1996).*

7. *Gray, G. T., "Classic Split-Hopkinson Pressure Bar Technique," LA-UR-99-2347, Los Alamos National Laboratory, Los Alamos, NM 87545. (1999). To be published in ASM Volume 8, Chapter 6A- Mechanical Testing, ASM International, Materials Park, OH, 44073.*

8. *Gray, G. T. and Blumenthal, W. R., "Split-Hopkinson Pressure Bar Testing of Soft Materials," LA-UR-99-4878, Los Alamos National Laboratory, Los Alamos, NM 87545. (1999). To be published in ASM Volume 8, Chapter 6E- Mechanical Testing, ASM International, Materials Park, OH, 44073.*

9. *Yadav, S. Chichili, D. R. and Ramesh, K. T., "The Mechanical Response of a 6061-T6 Al/Al2O3 Metal Matrix Composite at High Rates of Deformation," Acta metall. Mater., 43, 4453-4464, (1995).*

10. *Ravichandran, G. and Subhash, G., "Critical Appraisal of Limiting Strain Rates for Compression Testing of Ceramics in a Split Hopkinson Pressure Bar," J. Am. Ceram. Soc. 77, 263-267, (1994).*

11. *Rogers, W. P. and Nemat-Nasser, S., "Transformation Plasticity at High Strain Rate in Magnesia-Partially-Stabilized Zirconia," J. Am. Ceram. Soc. 73, 136-139, (1990).*

12. *Chen, W. and Ravichandran, G., "Dynamic Compressive Failure of a Glass Ceramic Under Lateral Confinement," J. Mech. Phys. Solids 45, 1303-1328, (1997).*

13. *Pettijohn,* E. R., *Sedimentary Rocks*, 3rd edition. Harper and Row, New York, (1975).

14. Podnieks, E. R., Chamberlain, P. G., and Thill, R.E. (1972). Enviornmental effects on rock properties. In Proceedings of Tenth Symposium on Rock Mechanics. American Institute of Mechanical Engineers, New York, 215-241.

15. Frew, D. J., Forrestal, M. J. and Chen, W., "Pulse Shaping Techniques for Testing Brittle Materials with a Split Hopkinson Pressure Bar," (Work in Progress).

16. Graff, K. F., Wave Motions in Elastic Solids. Dover, New York, (1975).

17. "Properties and Selection : Nonferrrous Alloys and Pure Metals," In Metals Handbook, 9th Edition, 2, American Society for Metals, Metals Park, OH, (1979).

Figure Titles

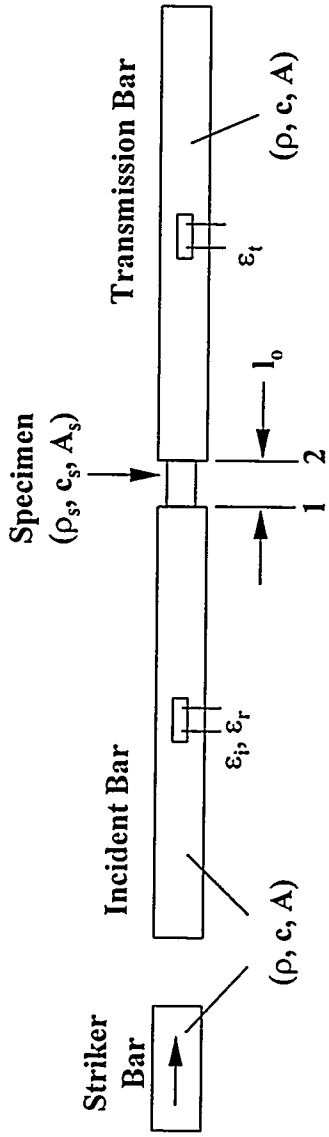
Striker Bar
(ρ, c, A)
Incident Bar
$\varepsilon_i, \varepsilon_r$
Specimen
(ρ_s, c_s, A_s)
1
2
l_o
ε_t
Transmission Bar
(ρ, c, A)

Fig.1

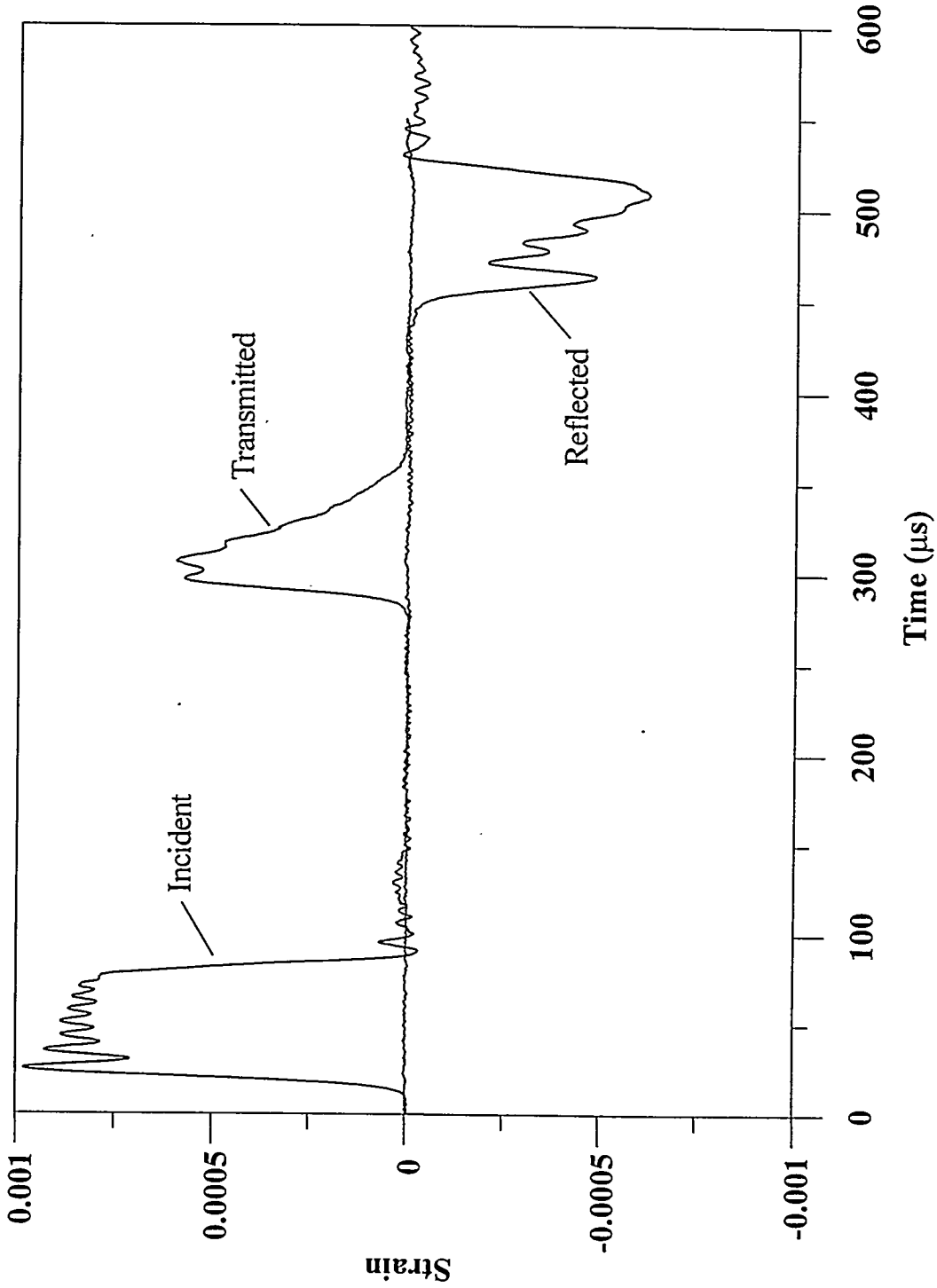
Incident
Transmitted
Reflected
Strain
0.001
0.0005
0
-0.0005
-0.001
0
100
200
300
400
500
600
Time (μs)

Fig. 2

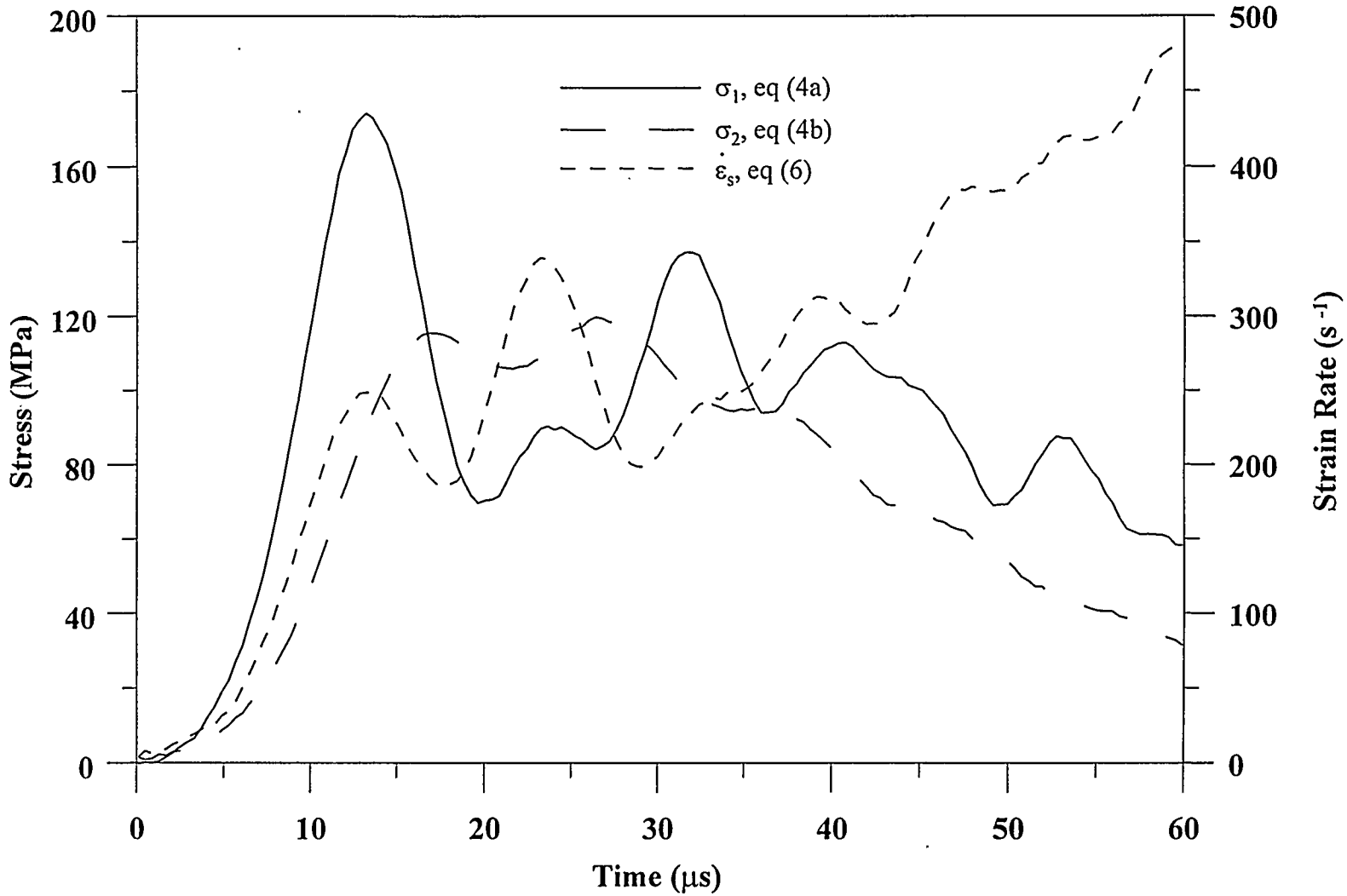
200
160
120
80
40
0
Stress (MPa)
500
400
300
200
100
0
Strain Rate (s^{-1})
0
10
20
30
40
50
60
Time (μs)
σ_1, eq (4a)
σ_2, eq (4b)
$\dot{\varepsilon}_s$, eq (6)

Fig. 3

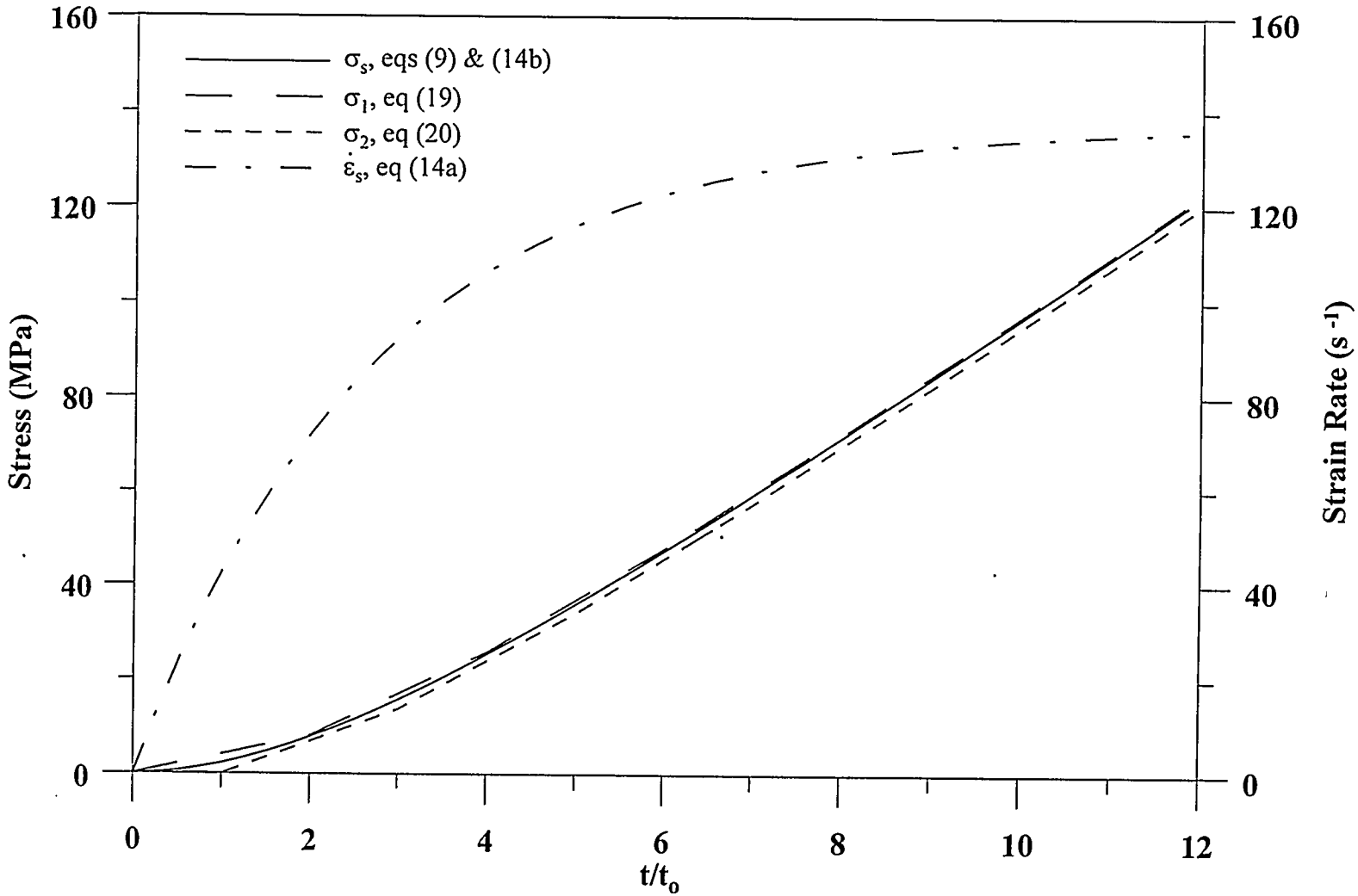
160
120
80
40
0
Stress (MPa)
σ_s, eqs (9) & (14b)
σ_1, eq (19)
σ_2, eq (20)
$\dot{\varepsilon}_s$, eq (14a)
0
2
4
6
8
10
12
t/t_o
Strain Rate (s^{-1})

Fig. 4

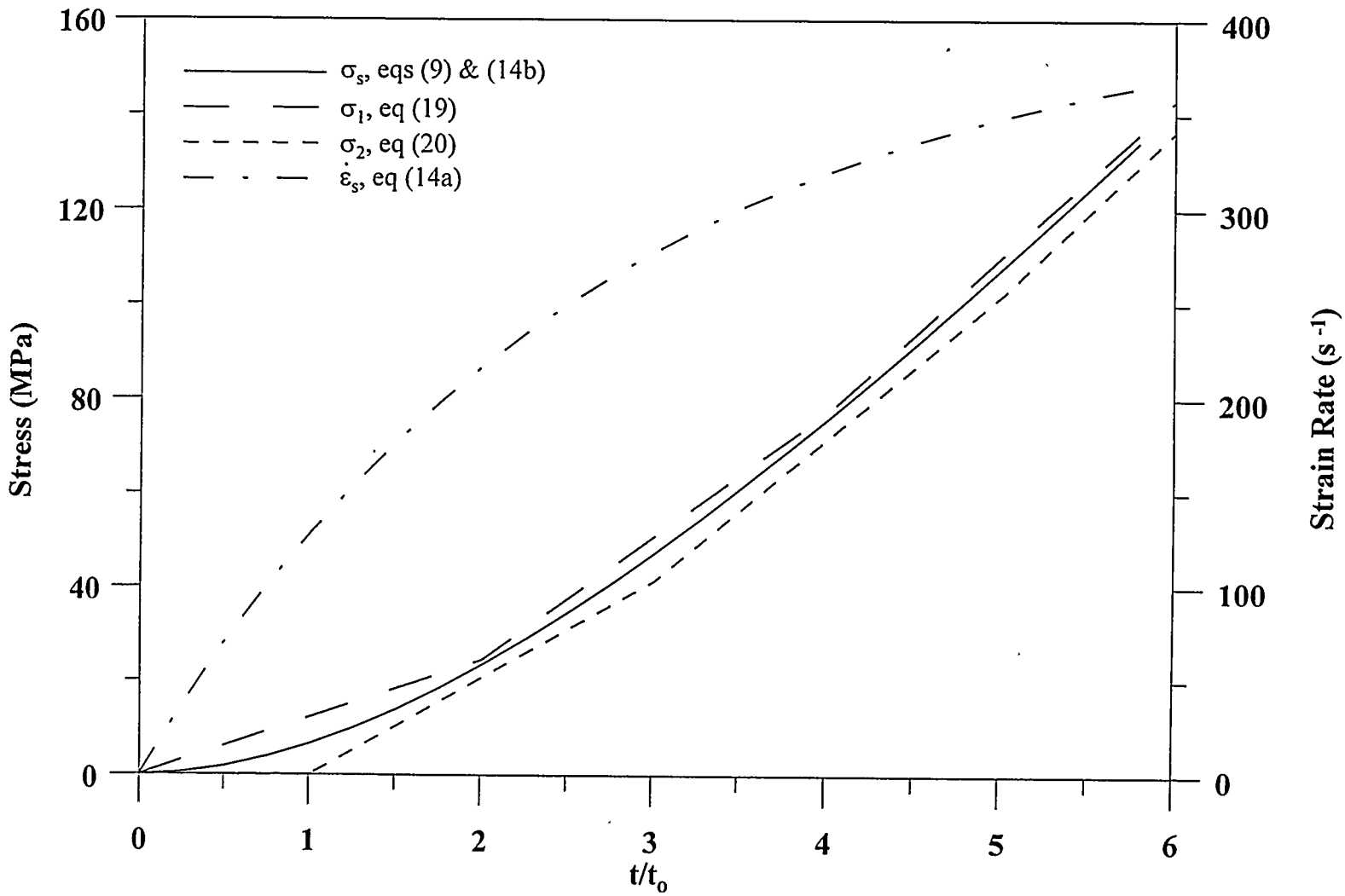
160
120
80
40
0
400
300
200
100
0
0
1
2
3
4
5
6
Stress (MPa)
Strain Rate (s -1)
t/t o
σs, eqs (9) & (14b)
σ1, eq (19)
σ2, eq (20)
ε̇s, eq (14a)

Fig. 5

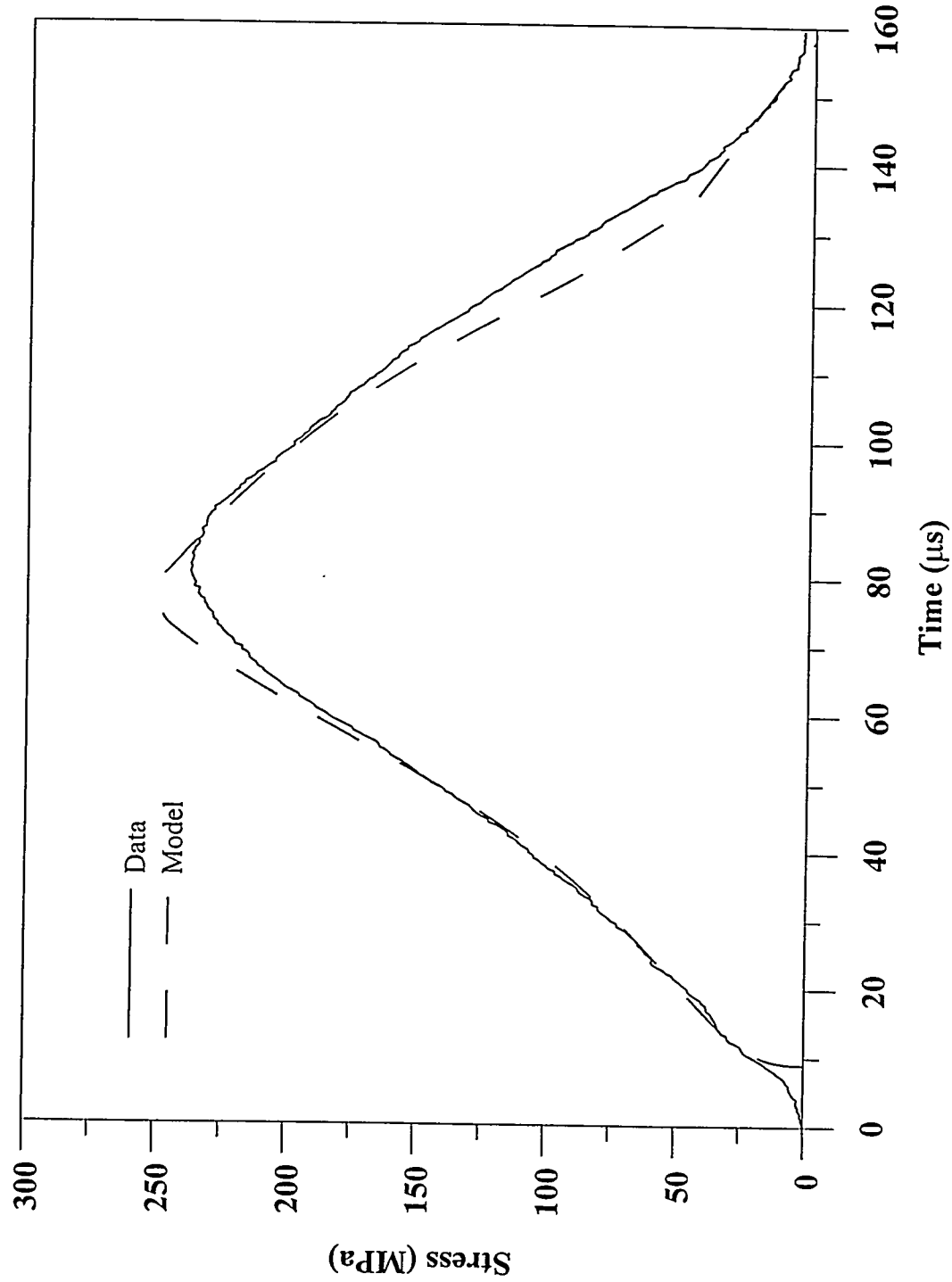
Stress (MPa)
300
250
200
150
100
50
0
0
20
40
60
80
100
120
140
160
Time (μs)
Data
Model

Fig. 6

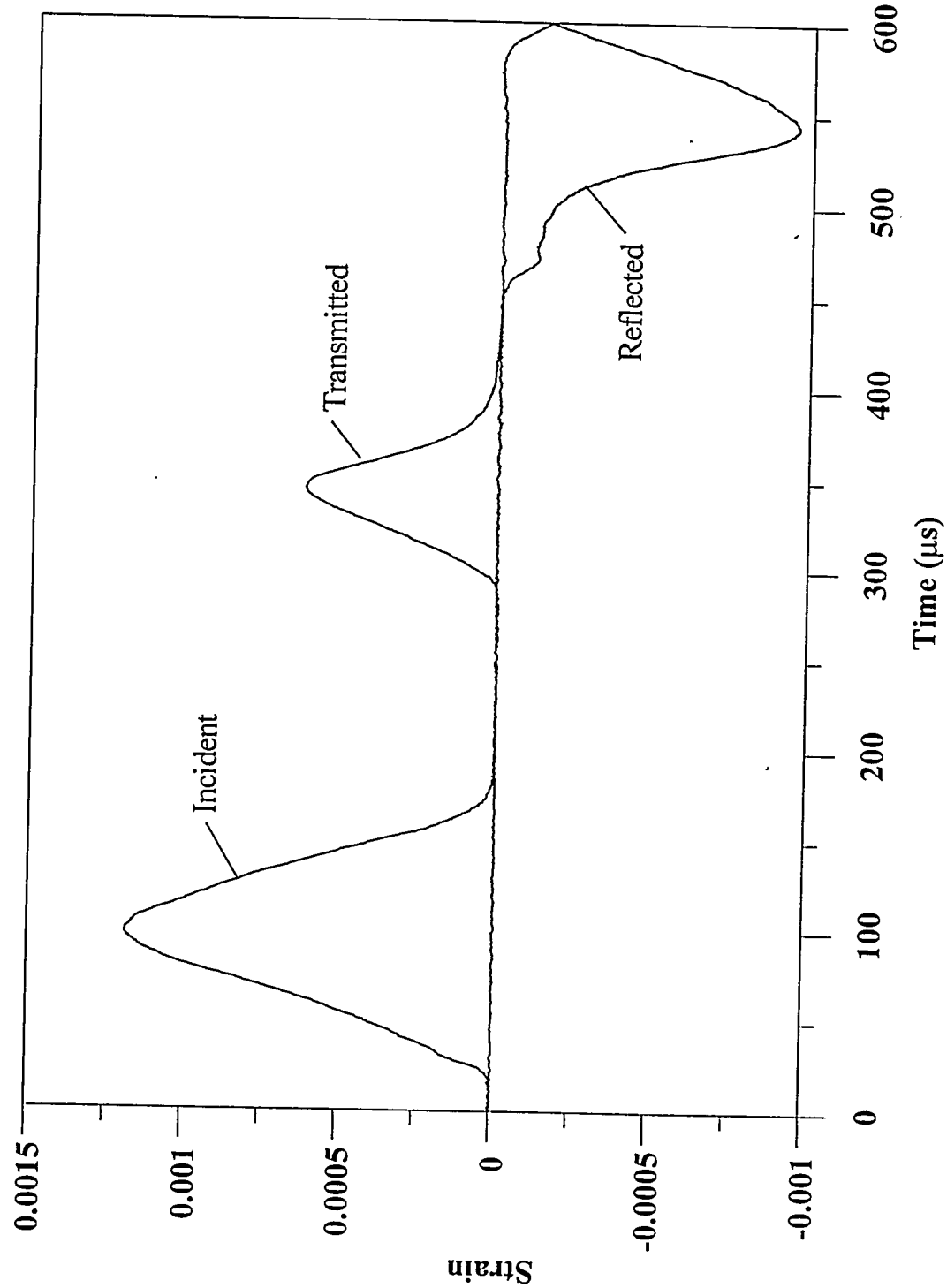
Incident
Transmitted
Reflected
Strain
Time (μs)
0.0015
0.001
0.0005
0
-0.0005
-0.001
0
100
200
300
400
500
600

Fig. 7

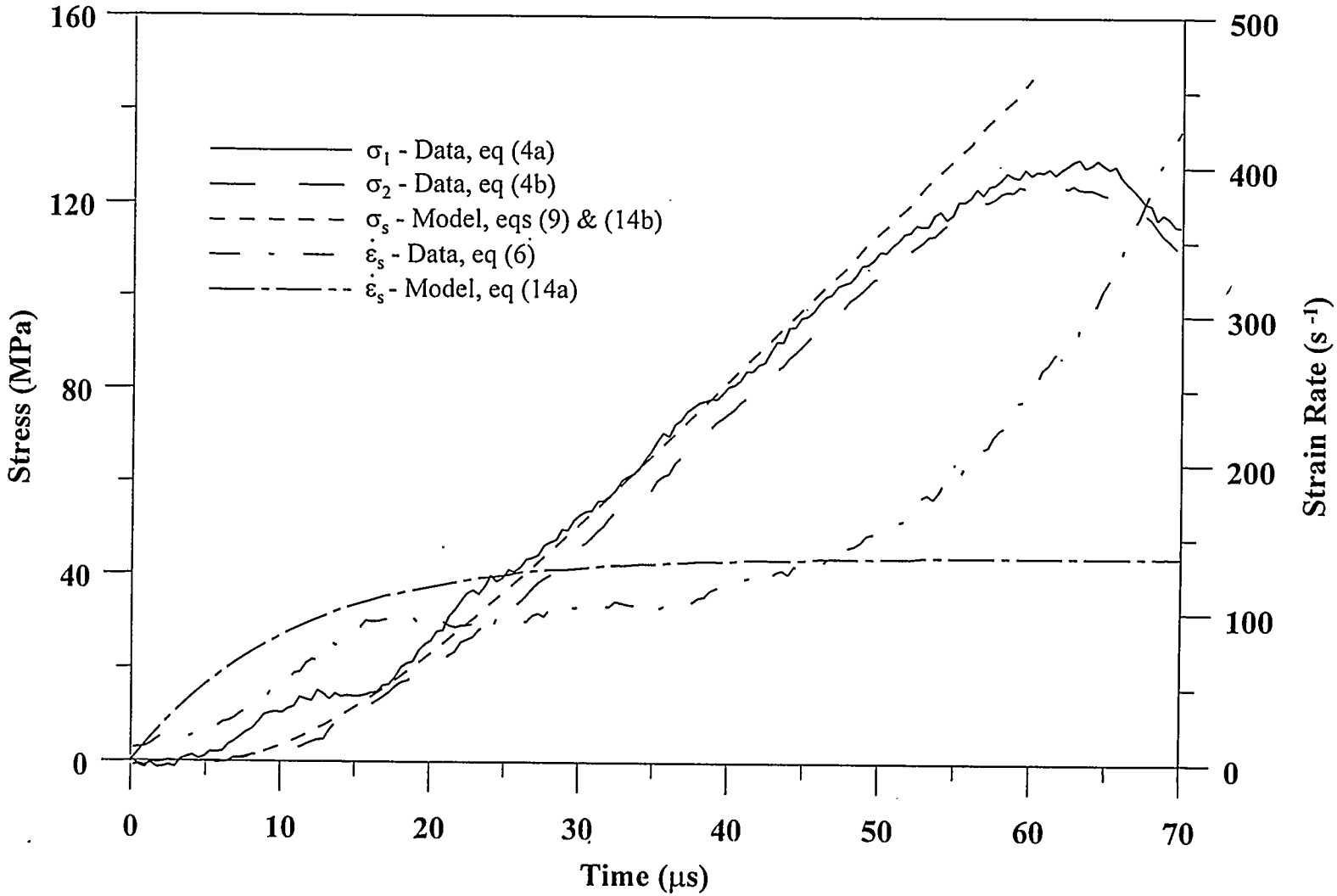
160
120
80
40
0
Stress (MPa)
500
400
300
200
100
0
Strain Rate (s-1)
0
10
20
30
40
50
60
70
Time (μs)
σ1 - Data, eq (4a)
σ2 - Data, eq (4b)
σs - Model, eqs (9) & (14b)
ε̇s - Data, eq (6)
ε̇s - Model, eq (14a)

Fig. 8

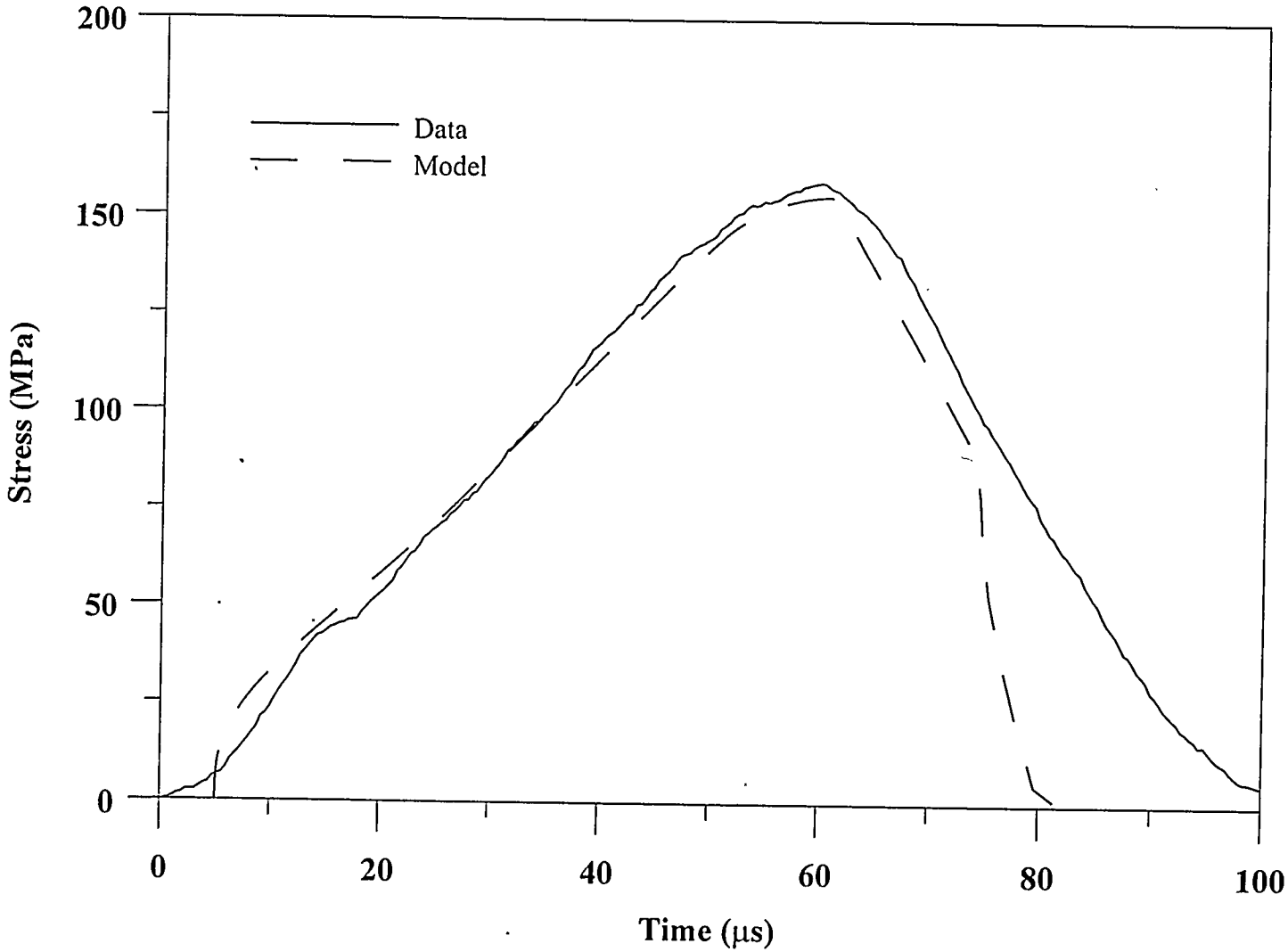

Fig. 9

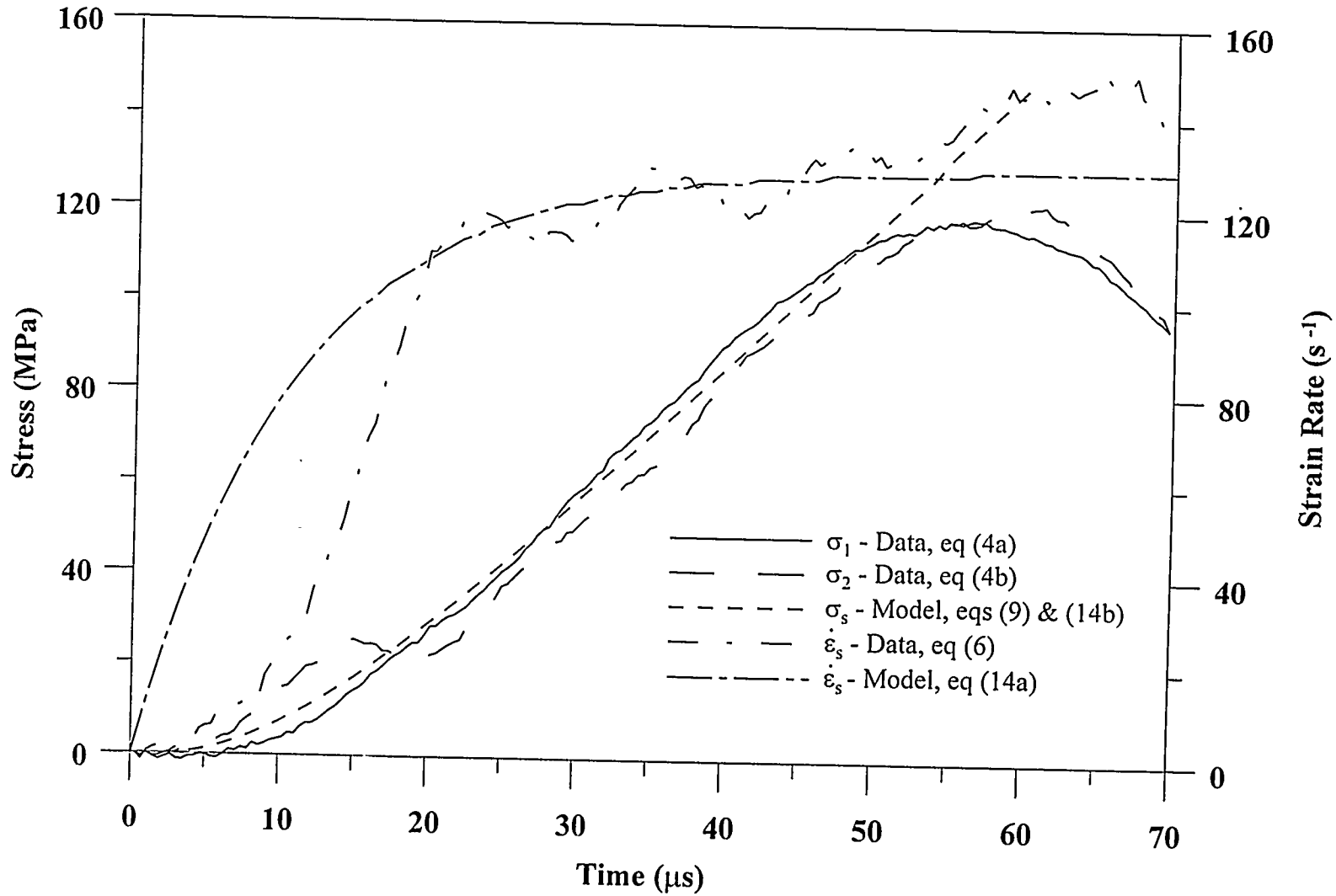
160
120
80
40
0
Stress (MPa)
160
120
80
40
0
Strain Rate (s -1)
0
10
20
30
40
50
60
70
Time (μs)
σ1 - Data, eq (4a)
σ2 - Data, eq (4b)
σs - Model, eqs (9) & (14b)
ε̇s - Data, eq (6)
ε̇s - Model, eq (14a)

Fig. 10

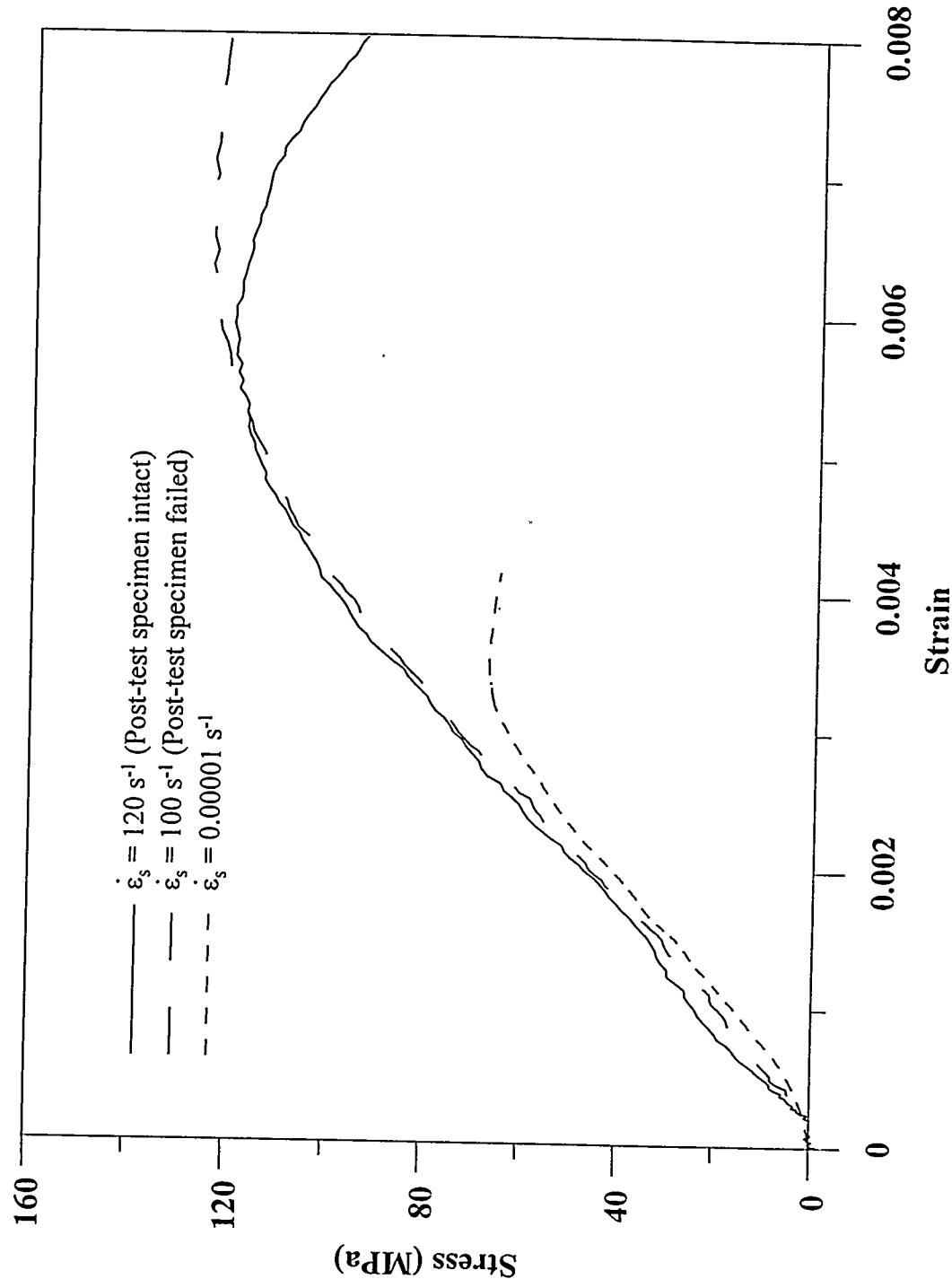
Stress (MPa)
160
120
80
40
0
0
0.002
0.004
0.006
0.008
Strain
$\dot{\varepsilon}_s$ = 120 s^{-1} (Post-test specimen intact)
$\dot{\varepsilon}_s$ = 100 s^{-1} (Post-test specimen failed)
$\dot{\varepsilon}_s$ = 0.00001 s^{-1}

Fig. 11